

# A New Deep-learning-Based Approach For mRNA Optimization: High Fidelity, Computation Efficiency, and Multiple Optimization Factors

Zheng Gong<sup>1†</sup>, Ziyi Jiang<sup>1†</sup>, Weihao Gao<sup>1</sup>, Deng Zhuo<sup>1</sup>, Lan Ma<sup>1,\*</sup>

<sup>1</sup>Tsinghua University, Tsinghua Shenzhen International Graduate School, Shenzhen, China.

\*corresponding author: Lan Ma (malan@sz.tsinghua.edu.cn).

<sup>†</sup>These authors contributed equally to this work.

## Abstract

The mRNA optimization is critical for therapeutic and biotechnological applications, since sequence features directly govern protein expression levels and efficacy. However, current methods face significant challenges in simultaneously achieving three key objectives: (1) fidelity (preventing unintended amino acid changes), (2) computational efficiency (speed and scalability), and (3) the scope of optimization variables considered (multi-objective capability). Furthermore, existing methods often fall short of comprehensively incorporating the factors related to the mRNA lifecycle and translation process, including intrinsic mRNA sequence properties, secondary structure, translation elongation kinetics, and tRNA availability. To address these limitations, we introduce **RNop**, a novel deep learning-based method for mRNA optimization. We collect a large-scale dataset containing over 3 million sequences and design four specialized loss functions, the GPLoss, CAILoss, tAILoss, and MFEloss, which simultaneously enable explicit control over sequence fidelity while optimizing species-specific codon adaptation, tRNA availability, and desirable mRNA secondary structure features. Then, we demonstrate RNop's effectiveness through extensive in silico and in vivo experiments. RNop ensures high sequence fidelity, achieves significant computational throughput up to 47.32 sequences/s, and yields optimized mRNA sequences resulting in a significant increase in protein expression for functional proteins compared to controls. RNop surpasses current methodologies in both quantitative metrics and experimental validation, enlightening a new dawn for efficient and effective mRNA design. Code and models will be available at <https://github.com/HudenJear/RPLoss>.

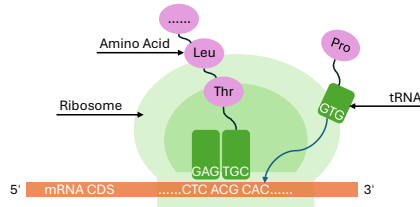
## 1 Introduction

The design and optimization of messenger RNA (mRNA) sequences represent a critical consideration in modern biological and biomedical research, primarily because the sequence dictates translational efficiency and subsequent protein yield. Historically, the need for mRNA optimization arose from challenges in achieving robust heterologous expression of target genes. This optimization is now indispensable for a wide array of biotechnological goals, encompassing large-scale protein production, the development of gene and cell therapies, synthetic biology circuits, and regenerative medicine strategies. The performance of mRNA molecules as therapeutic agents or research tools hinges on their sequence characteristics, directly impacting efficacy and production scalability. Moreover, for newly designed proteins lacking natural mRNA counterparts, computational sequence optimization is a prerequisite for achieving functional expression levels. Advancements in mRNA optimization also contribute to recombinant protein manufacturing and drug discovery pipelines [1]. Given the expanding therapeutic and industrial applications of mRNA [2], refining optimization techniques remains an area of intense investigation.

**(a) mRNA structure and codon**



**(b) Translation process of protein**



**Factors may influence protein expression**

1. Coding protein fidelity after optimization
2. Codon species adaptiveness: CAI
3. mRNA secondary structure: MFE
4. tRNA decoding affinity: tAI

**Fig. 1: Protein expression levels are significantly influenced by intrinsic properties of mRNA sequences and dynamics of the translation process.**  
(1) The coded protein shall be the same after optimization; (2) mRNA codon properties, such as codon usage bias and GC content; (3) the stability of mRNA secondary structures, manifesting in minimum free energy; (4) the kinetics of translation elongation, potentially quantified by tRNA pool composition, including tRNA isoacceptor abundance, summarized by a tRNA adaptation index.

While untranslated regions like 5'UTR, 3'UTR, and the poly(A) tail contribute to mRNA stability and translational control, the mRNA CDSs are the central functional components, as they dictate the amino acid sequences of encoded proteins, as depicted in Fig.1. Meanwhile, it is within the CDS that the codon-anticodon pairings with tRNA occur during translation elongation. Furthermore, CDS structure and composition (secondary structure and codon usage patterns) can influence co-translational protein folding dynamics [3]. Consequently, optimizing CDSs is the primary focus of most works aimed at enhancing protein expression from mRNA.

Meanwhile, overall protein expression levels can be determined by multiple factors, including intrinsic mRNA sequence properties, secondary structure, translation elongation kinetics, and tRNA availability. To quantify and optimize these factors, particularly within the crucial CDS region, several metrics and design principles are employed, including the Codon Adaptation Index (CAI) [4], GC content [5], the tRNA Adaptation Index (tAI) [6, 7], local Minimum Free Energy (MFE) calculations for secondary structure prediction [8–10], estimations of translation speed like the Mean of the Typical Decoding Rates (MTDR) [11], and sequence modifications such as uridine depletion [12–14]. Researchers utilize these indices and parameters to evaluate existing sequences, predict potential expression outcomes, and guide the rational design of optimized mRNA constructs through approaches like codon optimization [15].

The application of computational algorithms and machine learning techniques has significantly advanced the fields of codon optimization and de novo mRNA sequence design. However, despite considerable research efforts, persistent challenges limit the development and efficacy of advanced mRNA optimization methods, particularly those leveraging algorithms and deep learning.

Current mRNA optimization algorithms can be evaluated based on several key criteria: (1) **fidelity** (preventing unintended amino acid changes), (2) **computational efficiency** (speed and scalability), and (3) **the scope of optimization variables considered** (multi-objective capability).

Firstly, maintaining sequence fidelity is the most important requirement. For mRNA optimization, most of its procedures strictly preserve the original amino acid sequence by only introducing synonymous codons. Non-synonymous changes, sometimes called 'protein mutation', yield unintended protein variants and are generally unacceptable. Some deterministic algorithmic approaches like Dynamic Programming (DP) or lattice parsing can guarantee synonymous substitutions [16, 17]. However, ensuring complete fidelity remains a significant challenge for many machine learning models, especially for probabilistic models, which may randomly introduce non-synonymous mutations. For instance, such mutations can be a potential risk in generative models. Language models like Evo2 [18] can hardly restrict their occurrence. Other deep learning architectures like BiLSTMs or RNNs applied to this task [1, 19, 20] also have possible mutations.

Secondly, computational efficiency dictates the throughput and feasibility of applying optimization algorithms, especially for large-scale studies or long sequences. Deep learning methods often exhibit extraordinary computational efficiency, with typical computation times increasing linearly with sequence length, enabling rapid optimization [1, 19, 20]. Simple, single-factor optimization strategies (e.g., greedy algorithms

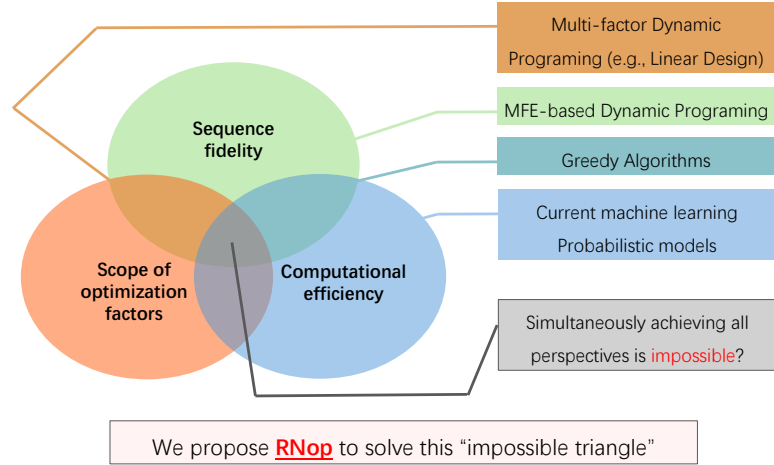


**Fig. 2: The "Impossible trinity" of mRNA optimization.** Simultaneously achieving high sequence fidelity, computational efficiency, and a wide range of optimization factors remains a significant challenge for current mRNA design methods. However, in this paper, we propose a new deep learning based method to achieve all factors above.

maximizing CAI) also offer very high speed but are inherently limited by the narrow scope of variables. Conversely, strict algorithmic methods like DP [13, 16, 17, 21] are much more rigid and cumbersome. While they enable considering optimality for multiple factors, they can be computationally intensive. Despite optimization efforts, their runtimes can range from minutes to hours for longer sequences, hindering potential high-throughput applications compared to the faster execution times of deep learning approaches.

Thirdly, the scope of optimization factors incorporated into the algorithm critically influences the quantitative metrics of the designed mRNA, which can be related to *in vivo* performance. Many methods, including earlier single-factor approaches and even some DP implementations [13, 16, 21], consider a limited set of variables. The development of LinearDesign [17] is famous for its progress in integrating CAI and MFE simultaneously and achieving great performance. This combination of optimization factors is still insufficient due to a lack of consideration of the translation process. Furthermore, many deep learning approaches learn complex patterns directly from natural sequence data, often only containing latent knowledge. They may lack mechanisms for the explicit integration of prior knowledge like other aforementioned algorithms do, posing challenges for interpretability and ensuring adherence to specific design constraints [19, 20]. However, as previously stated, protein expression is modulated by a complex interplay of factors, from mRNA sequence features to translation dynamics and RNA structure. In summary, while progress has been made, the scope of optimization factors addressed by most current methods remains limited compared to the full spectrum of biological determinants governing mRNA function.

The analysis above indicates that simultaneously achieving high sequence fidelity, computational efficiency, and a wide range of optimization factors remains a challenge for current mRNA design methods. This interplay often forces trade-offs, like a phenomenon conceptually illustrated by the "optimization trinity" depicted in Fig. 2. However, in this work, we introduce **RNop**, a novel deep learning framework designed to concurrently address these objectives. RNop allows simultaneous optimization of mRNA sequences, demonstrating remarkable improvements in fidelity guarantees, computational speed, and the factors considered, thereby enabling new possibilities for protein expression optimization across various species and *de novo* protein and mRNA design.

We developed RNop to optimize mRNA CDS by integrating explicit, multi-objective optimization and precise fidelity control within a deep learning architecture. Specifically, the RNop framework utilizes Transformer-based models and special tokenization methods to optimize mRNA CDS regions for diverse target species.

The development and application of four novel loss functions specifically designed for deep learning-based mRNA optimization is the core of RNop models: GPLoss, CAILoss, tAILoss, and MFEloss. It is these loss functions that guide the optimization process to enhance sequence suitability for a target species, improve predicted mRNA stability, and ensure sequence fidelity, thereby addressing key aspects of translation efficiency and the mRNA lifecycle.

**Sequence suitability:** The CAILoss focused on enhancing sequence suitability for a target species. It optimizes for the codon usage bias of the target organism, guiding the model towards codons frequently utilized in that species' transcriptome.

**Translation efficiency:** The tAILoss focused on enhancing translation efficiency. Similar to the CAILoss, the tAILoss promotes codons corresponding to abundant tRNA anticodons within the target species, aiming to improve translation elongation efficiency through enhanced tRNA adaptation.

**Minimizing free energy:** The MFEloss integrates secondary structure considerations by minimizing the predicted MFE of mRNA sequences, which is calculated by loss models specially trained for MFE prediction. Lower MFE values have been linked to increased mRNA stability and potentially longer half-lives [9, 10].

**Synonymous sequence preservation:** The GPLoss is specifically designed to control sequence fidelity. Penalizing non-synonymous codon changes during the optimization process enables the RNop models to enforce the original amino acid sequence. Therefore, it can effectively prevent undesired mutations in the resulting mRNA sequence when required.

Then we collected an mRNA sequences dataset containing over 3,000,000 mRNA sequences for training, validation, and testing. Compared to 38000[20], 42266[1], or 71820[22], the amount of mRNA sequences is larger than previous codon optimization methods. A transformer-based model, named RNop model, is also designed for mRNA optimization. The RNop models leverage the Transformer architecture and treat the mRNA optimization tasks as image-to-image translation in computer vision.

We conducted numerous experiments on the collected datasets and proposed models. Extensive *in silico* and *in vivo* experiments validate that our methods are effective

for mRNA optimization. The RNop exhibits great efficiency in terms of time and computational consumption. The in silico results demonstrate an escalation in all factors related to protein expression. On the test datasets and proteins for subsequent biological experiments, there is no mutation is observed in the coded aa sequences of optimized mRNA sequences. Meanwhile, the biological results substantiate the higher protein expression in multiple ways. We conducted experiments on fluorescent proteins (functional proteins) and the COVID-19 spike protein (vaccine-related protein), in which results we observed protein expression promotion up to 4.6 times higher than the original ones. We compared our methods to current codon optimization and mRNA design methods, and the results show that RNop surpasses current methods both in in silico and in vivo experiments. We will release the demonstration and source code for further research in the future.

Our contributions can be summarized as follows:

- We introduce **RNop**, a novel deep learning framework for mRNA optimization designed to simultaneously address sequence fidelity, computational efficiency, and multi-objective optimization across a broad range of factors.
- We develop four novel loss functions according to the mRNA lifecycle: GPLoss, MFEloss, CAILoss, and tAILoss. They can achieve controlling sequence fidelity, enhancing structural stability via Minimum Free Energy, and species-specifically improving translation efficiency.
- The effectiveness of RNop is demonstrated through extensive *in silico* analysis and validated by *in vivo* experiments. Optimized sequences generated by RNop show prominent improvements in quantitative metrics and achieved over a significant increase in protein expression for functional proteins compared to controls/baselines.
- The proposed RNop framework offers significant advantages in computational speed and suitability for batch processing, achieving throughputs of up to 47.32 sequences/s.

## 2 Related Works

### 2.1 mRNA design

The design of mRNA originates from the biological synthesis of mRNA. There are many biological ways to design the mRNA, such as mutation[23], replacement[24, 25], and statistical analysis[26]. Though they have obtained significant results, much time is required for a careful and rational design to produce a delicate sequence. According to the experiments and experience, the codon adaptation index (CAI)[4] and tRNA adaptation index (tAI)[6, 7] were proposed. These indices are widely used in codon optimization and mRNA design[15]. The emerging algorithm methods also regard them as important factors [16, 17, 19].

After optimization, the mutation (the change of coded amino acid) of protein sequences might happen when the probabilistic algorithm models are applied. Therefore, to prevent the sequences from mutation, most methods of designing an mRNA sequence use dynamic programming (DP). The DP models only replace the codons

within the synonymous codons, thus ensuring that the models generate sequences coding the same protein sequences. Mathews et al.[8, 27] summarized the nearest neighbor parameters for the DP method to optimize the mRNA with its MFE. Then the DP methods have been increasingly developed through the years, and the RNAStructure [28] and the  $N^6$ -methyladenosine update [29] make the prediction and optimization of RNA structure based on the MFE much more precise. The modification of Goro Terai et. al[16] improved the time complexity of mRNA sequences of length  $n$  from  $O(n^3)$  to  $O(W^2 \times n)$  by limiting the maximum distance between base-paired nucleotides  $W$ . Akito Taneda[21] et al. applied the constrained Pareto-optimal solutions to accelerate the DP algorithm. LinearDesign[17] is a significant milestone for algorithm-based mRNA optimization. It leverages the CAI and MFE as main factors to optimize the mRNA sequences and successfully reduce the time complexity by simplifying the DP to lattice parsing. Nikita et al.[13] utilized the DNA Chisel[14] to build an open-source DNA (and mRNA) optimization platform.

However, the rise of machine learning and deep learning methods also grew rapidly after the 2010s. Using deep learning methods can not avoid the mutation problem mentioned above, as most deep learning methods are probabilistic models. Fu et al.[19] proposed the BiLSTM-CRF to optimize the CAI of mRNA. Their method considers only CAI for higher expression, and the mutated codons will be replaced by the original ones to ensure protein consistency. Recurrent Neural Networks (RNNs) suit the sequence-to-sequence tasks well, and Goulet et al.[20] and Jain et al.[1] used RNNs to optimize codons for hamsters and *E. coli*. They use the protein sequences as inputs and original mRNA sequences as targets to train the models to generate native-like and high-CAI sequences. Gong et al.[30] demonstrated a new method leveraging BiLSTM-CRF for optimizing mRNA sequences with UTRs.

Large language models (LLMs) are also utilized in the mRNA design. Nicole et al.[22] applied BERT[31] for low-expression gene prediction. The CodonBert[32] is an LLM pre-trained for multiple tasks related to mRNA. It achieved competitive performance in many tasks but lacked in vivo experiments.

## 2.2 mRNA-related tasks

Algorithms like DP, machine learning, or deep learning-based methods have been used for RNA-related data analysis like structure and function prediction[33, 34] for a long time. However, most existing work focuses on improving the performance of artificial intelligence in different supervised RNA tasks, including classification or regression[35–38]. Since the flourishing of deep learning, researchers have attempted to use deep learning models to predict the function or 3D structure of RNA [39–43]. In addition to classical convolutional neural networks or language models, researchers have also applied the methods of large language models to these benchmark RNA tasks. Specifically, researchers improved the performance of the model in downstream RNA tasks by pre-training with large-scale RNA data[32, 40, 40].

The exponential growth of high-throughput sequencing technologies has generated a large number of unannotated RNA sequences, while the lack of sufficient annotation data and 3D structural information limits the study of these RNAs. Therefore, many datasets were found for further research. The Stanford OpenVaccine dataset and

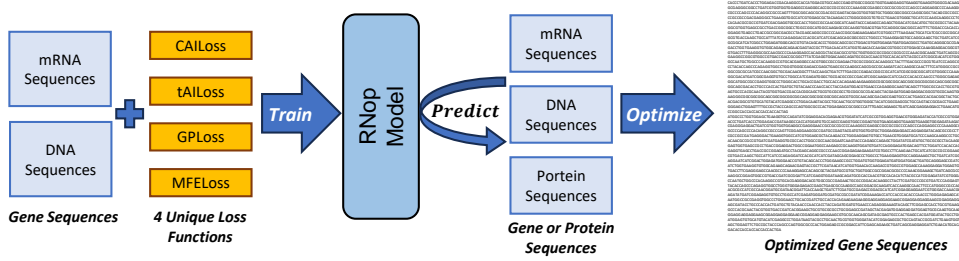


**Fig. 3: The framework of our optimization methods:** Our methods include the coding method, 4 different loss functions, and a new Transformer-based deep learning model. (1) The coding method can encode multiple kinds of gene sequences into uniformly formatted feature maps. (2) The 4 unique loss functions can be applied in various types of deep learning models. (3) The new method, RNop model, can process the sequence features using Vision Transformer structures. The optimized sequences exhibit great expression improvements in both computerized and in vivo experiments.

competition on Kaggle achieved more stable and efficient COVID-19 vaccines through crowdsourcing and collaborative design within 6 months [44, 45]. The *E. coli* proteins dataset [46] comprises experimental data for protein expression in *E. coli*, which are labeled as low, medium, or high expression. The mRNA stability dataset [47] includes thousands of mRNA stability profiles obtained from human, mouse, frog, and fish. The purpose of these datasets is to facilitate the design of algorithms for predicting the stability of mRNA, thereby providing AI-assisted evaluation tools for protein expression levels.

### 3 Method and Implementation

Our methods include the coding method, 4 different loss functions, and a new Transformer-based deep learning model. The coding method is the cornerstone of our method. With this coding rule, we are able to transfer the mRNA CDS to a coding probability space and thus can encode multiple kinds of gene sequences into uniformly formatted feature maps.

Then, to leverage the prior knowledge from the biolocal indices, we create four different loss functions for the RNA deep learning training process: GPLoss, CAILoss, tAIloss, and MFEloss. They are formulated with linear algebra from the method above and deployed with CAI or tAI parameters, and thus can be integrated into deep learning methods.

Furthermore, the new method, RNop model, is designed for the ability to optimize the mRNA CDS with flexibility in different optimization factors. Notably, it can process the sequence features using Vision Transformer structures. The trained RNop model can handle gene or protein sequences and provide optimized gene sequences.

The frameworks of our methods are shown in the flowchart, Fig.3.

### 3.1 Coding Rules

To standardize mRNA sequences as input for neural networks, we designed a coding rule that converts CDS sequence data into numerical matrices. While some large language models use tokenizers, and there are coding methods like K-mers[48], they can be redundant and cumbersome because there are only limited mRNA codons, and the vocabulary is relatively small. Therefore, we propose a new coding method for converting mRNA sequences into matrices.

Generally, the mRNA sequences consist of four nucleic acids: A, U, C, and G. Meanwhile, most RNA datasets (including the data downloaded from NCBI[49] datasets) use "T" to replace "U" to keep the representation the same as the DNA sequences. Thus, following the typical order of "TCAG," we represent RNA sequences accordingly and include both mRNA and DNA CDS. Therefore, with fixed order and 3 nucleic acid positions in one codon, the vocabulary of this coding rule is  $4^3 = 64$ . The position of each codon in this vocabulary is fixed, which enables us to map one codon to its coding protein and then to its coding probability space for anonymous codons. The detailed mapping method of this coding rule can be referred to Appendix.A.

Additionally, sequences with unknown or uncertified codons are denoted as "N" or "RYMKSWHBVDN." With five alphabets representing RNA, the vocabulary size is  $5^3 = 125$ . Although using more alphabets (e.g., RYMKSWHBVDN) provides richer information than a singleton "N," it would inflate the vocabulary size to  $15^3 = 3375$ . That could be an unworthy choice as they are really rare in the sequences.

Furthermore, RNA sequence lengths vary a lot. Alongside the 125 codon symbols, we introduce an  $<EOS>$  (End Of Sequence) symbol at the end of RNA sequences. To ensure consistent input and output lengths for neural networks, we also propose adding a  $<PAD>$  (Padding) coding symbol. These tokens can extend RNA sequences to a specified maximum length. With fixed lengths, it will be possible to apply conventional convolutional networks, vision models, or any neural networks with fixed input sizes for mRNA data processing.

### 3.2 GPLoss

The mutation means the sequence after optimization has codons that are not synonymous at the same position, resulting in coding for different proteins. As most deep learning and neural network models are probabilistic models, it is common for them to generate codons with different coding proteins if there is no constraint. Meanwhile, as mentioned in Section.2.1, algorithm methods use DP[16] or lattice parsing[17] rather than probabilistic models to avoid mutation, while some deep learning methods replace the mutated codons with the original ones to avoid mutation[19]. However, some of the mutations will not affect the function of proteins. Sometimes the mutations may exhibit desired features that the original ones do not possess. The controlled mutation is also an application scenario for mRNA design. Therefore, the GPLoss is designed to be flexible. The mutation rate can be regulated by different loss weights of GPLoss.

GPLoss follows the mapping process discussed in Section.3.1 with a variable loss weight. It allows the codons positioned in the correct possibility space, and rejects the codons in the incorrect possibility space with the penalty of loss value. Thus,

the GPLoss with high loss weight can give massive penalties for models when they generate a mutated codon. When needed, it can control the coding proteins of optimized sequences to keep them the same after the optimization process. Meanwhile, low GPLoss loss weight can allow models to generate mutation codons. With different loss weights, the mutation rate can vary from 0 to 100% under control.

In our models, the loss weight of the GPLoss is set to  $10^{-1}$ , which is significant enough to restrict the mutation rate to 0. We also conducted experiments to show how the mutation rate varies as the loss weight changes in Section 4.1.

### 3.3 CAILoss

According to the original CAI computation process[4], each codon has different CAI indexes for different species. Moreover, the preferred codons for specified species have the highest CAI indexes for each protein. Therefore, we design the CAILoss to encourage the optimization model to generate the codons with the highest CAI indexes. The detailed computation process of CAILoss and samples of its parameter matrix can be found in Appendix.B.

When using the CAILoss, we shall specify the species first. The parameters of CAILoss are initialized using different codon usage bias parameters from different species. We accessed the open-source database of the Genescrypt[50] to download the raw data. Currently, the CAILoss parameters of "ecoli", "yeast", "rat", "mouse", and "human" are provided in the source code. More species parameters can be updated easily by adding their codon usage bias index to the raw data.

### 3.4 tAILoss

The tAILoss specifically focuses on tRNA counts across different species, where the anticodons associated with the highest tRNA counts are considered the most preferred codons within DNA sequences. In this approach, we adhere to the classic tAI computation method using optimized parameters, as referenced in the literature[6, 7].

Though the computation process of the tAI suits linear algebra naturally, to suit our coding rule, there are minor adjustments. First, we alter the codon order of the original tAI computation according to the codon order in the input and output matrix. Then, the original presentation of anticodon is transferred to their corresponding codons. The detailed computation process of tAILoss and samples of its parameter matrix can be found in Appendix.B.

The tAILoss function can bias the optimization model toward generating codons with the highest tRNA anticodon counts. While this approach aims to improve the transfer RNA Adaptation Index (tAI), it may inadvertently impact RNA translation efficiency. Additionally, tAILoss is a species-specific loss function, with fixed parameters determined during the initialization process. In our source code, we provide tAI parameters for several species, including "ecoli", "yeast", "rat", "mouse", and "human." The raw tRNA count data is sourced from GtRNADB.[51]

### 3.5 MFELoss

To improve the minimum free energy of mRNA sequences, we designed the MFELoss for the RNop model. The MFELoss consists of a loss function model to predict the MFE of output mRNA sequences and a loss operation. Generally, the more stable the mRNA sequences are, the longer their half-life is, which indicates better expression time and amount in the cell[9, 10]. The CAI and tAI can only indirectly influence the MFE of mRNA sequences. Therefore, we designed the MFELoss to optimize it directly.

To calculate the MFE of mRNA sequences, there are methods using algorithms which are the  $O(N^3)$  time complexity [8, 17]. However, they can hardly be integrated into neural networks using linear algebra transformation, facilitating the gradient descent. Meanwhile, using these methods as a loss function will make the training process slow when the mRNA sequence is long. Therefore, to make MFE computation fast and utilizable in deep learning, we build a small loss network specialized to predict the MFE of mRNA sequences.

First, we calculate the MFE value in kJ/mol using RNAStructure[28] for all RNA sequences in our collected datasets. Though there are models [52] that can predict both the secondary structure and MFE of mRNA sequences, their functions are redundant for MFE calculation only. Therefore, a very small Multilayer Perceptron (MLP) neural network is used for this task. We tried different model sizes and found that a small model with only 12 layers and 5.4M parameters can do this job well. We selected this model as our loss model for the MFELoss. The calculation of MFELoss is shown in the Eq.1. The  $MFE_{i,gt}$  represents the ground truth MFE of the sequence  $i$ , and  $O_i$  represents the  $i$ th output of the optimization model. The  $F_{mfe}$  means the  $O_i$  is processed by the MFE model mentioned above. The  $\lambda \in [1, +\infty)$  is the MFE ratio to ensure the optimization target is higher than the original MFE. Consequently, the loss operation  $Loss$ , which can be selected from L1, SmoothL1, MSE, and Charbonnier loss, is applied to these vectors.

$$MFELoss = Loss(\lambda \times MFE_{i,gt}, F_{mfe}(Seq_i)) \quad (1)$$

The MFELoss makes the optimization model prone to generating mRNA sequences with better (lower) MFE. However, when compared to the other loss functions, the values of MFELoss are relatively higher. The optimization targets of the MFELoss are MFE values, which usually are in the  $10^2$  order of magnitude, while others are within  $(0, 1]$ . Therefore, the loss weight of the MFELoss is  $100\times$  lower than CAILoss or tAILoss.

### 3.6 mRNA Optimization Model: RNop

We designed a new optimization approach for the optimization tasks: a Transformer-based model named RNop. The RNop model is a sequence-to-sequence model that consists of Transformer and convolutional network layers. The mRNA sequences are simpler on the one hand– they usually have less vocabulary–and complicated on the other hand–they are more strict with length and coding. Therefore, the RNop model is designed specialized for this task with extensive experiments.

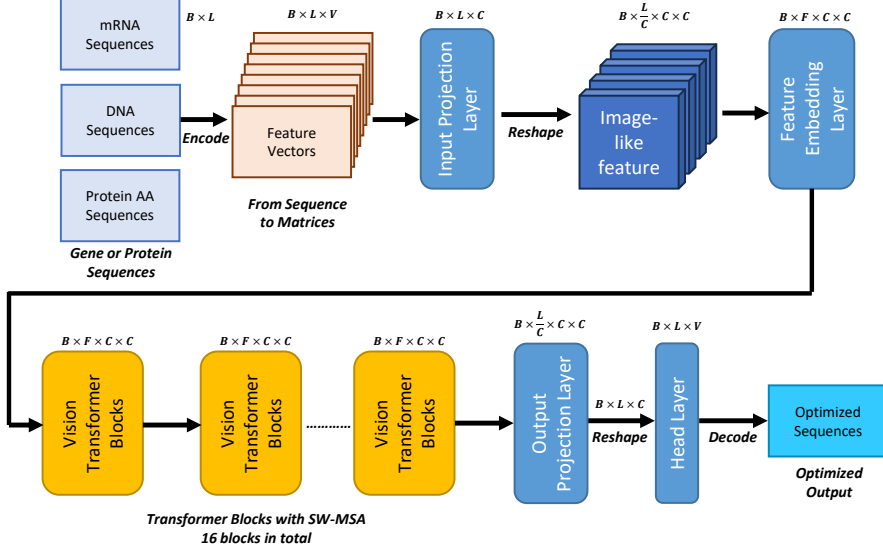


**Fig. 4: The architecture of our RNop model:** (1) RNop model uses our coding method to encode multiple kinds of gene sequences to feature matrices. (2) The feature matrices are processed and reshaped to image-like features. (3) Then, the model can process these features using Vision Transformer structures. (4) The features are unpacked and restored to sequences and decoded to desired optimal sequences.

The RNop model utilizes the Vision Transformer[53, 54] architecture to deal with the sequence-to-sequence task. Its architecture is shown in Fig.4. We assume the input sequences  $I$  have the shape of  $B \times L \times V$ , where the  $B$ ,  $L$ , and  $V$  represent the batch size, sequence length, and vocabulary size. As discussed above, we can choose  $TCAG$  or  $TCAGN$  coding for the mRNA, which consists of  $4^3$  or  $5^3$  vocabulary. Plus the  $<EOS>$  and  $<PAD>$ , the total vocabulary usually adds up to 66 or 127. Therefore, to standardize this, the input  $I$  is processed by an input projection layer to modify its shape to  $X_1 \in \mathbb{R}^{B \times L \times C}$ , where  $C$  represents the projection channel. The feature  $X_1$  is reshaped to  $X_2 \in \mathbb{R}^{B \times \frac{L}{C} \times C \times C}$ , which is exactly akin to an image with  $\frac{L}{C}$  channels, height  $C$  and width  $C$ .

Subsequently, the image-like feature is processed by a feature embedding layer, which is an overlapping convolutional layer with a stride of 1 and a kernel size of 3. This is due to we observed severe information loss if we applied the common non-overlapping patch embedding layer with a stride of 4 and a kernel size of 4. The processed feature is  $X_3 \in \mathbb{R}^{B \times F \times C \times C}$ , where  $F$  is the feature embedding dimension. Then,  $X_3$  is processed by 16 Shifted Window-based Multihead Self-Attention layers[54]. This attention mechanism ensures that the global feature and local feature can be extracted and fused. The feature size is kept the same during this process, and no downsampling or upsampling is applied. We call this process the ViT encoder. The output of the last WMSA layer is  $O_1 \in \mathbb{R}^{B \times F \times C \times C}$ . Then, the  $O_1$  is processed by a

point-wise convolutional layer changing its channel from  $F$  to  $\frac{L}{C}$  and further reshaped back to  $O_2 \in \mathbb{R}^{B \times L \times C}$ .

Consequently, we utilize a head layer to modify the last dimension of the  $O_2$  from  $C$  to  $V$  to give the final output  $O \in \mathbb{R}^{B \times L \times V}$ . Then the output can be decoded to mRNA sequences or used directly in the loss function calculation for gradient descent.

### 3.7 Dataset

The genome data is downloaded from the NCBI database. We downloaded the gene sequences of Eukaryota and Bacteria from the NCBI Genome Database[49]. All sequences dated to May 1th 2024 were downloaded. The virus genome data is downloaded from the NCBI Virus Database[55]. The sequences are filtered, and only the sequences that are complete and have lengths from 1 to 30000 were downloaded.

After collecting the dataset, we preprocess the sequences into the data sheets. In this step, the sequences are cropped to the UTRs and CDS sequences. The duplicated CDS sequences (mRNA) are deleted to avoid data leaking. We randomly sampled 2,000,000 sequences from each category: Eukaryota, Bacteria, and Virus. The sampled sequences are further divided into train, validation, and test sets, with partitions of 90%, 1%, and 9% respectively. There are 5,400,000 sequences in the training data, and 60,000 and 540,000 in the validation and test data.

### 3.8 Implementation Details

During training, the RNop model is applied with PyTorch version 2.1 and trained with CUDA version 12.2. We train each model for 120,000 iterations (equivalently 12 epochs) with a batch size of 32 and a learning rate of  $10^{-4}$  with cosine decay. The AdamW [56, 57] optimizer is applied with a 1000 iterations warm-up. All experiments are trained using a single NVIDIA GeForce RTX3090 GPU, running for 32 hours to complete the training process.

### 3.9 Quantitative Metrics

We utilize biological metrics to evaluate the optimality of output sequences.

The **CAI** is an extensively used metric for mRNA. As we have mentioned in the Section.3.3 and 2.1, its computation is based on the codon usage bias of different species. Therefore, we calculate the CAI of the original and optimized sequences to compare their optimality in the target species. The parameter and computation process follow the original literature[4, 50].

$$CAI = f_{CAI}(mRNASEquence). \quad (2)$$

The **tAI** is another metric for mRNA. The tAI, like the CAI, evaluates the anti-codon adaptability for mRNA sequences. As we have mentioned in the Section.2.1, its computation is based on the tRNA counts of different species. Therefore, we calculate the tAI to compare their tRNA affinity in the target species. The computation process follows the original literature[6, 7].

$$tAI = f_{tAI}(mRNASEquence). \quad (3)$$

The **MFE** is a chemical metric for mRNA. Lower MFE has been linked to increased mRNA stability and potentially longer half-lives [9, 10]. We use the RNAStructure[28] to calculate the minimum free energy of optimized mRNA sequences.

$$MFE = f_{MFE}(mRNASequence). \quad (4)$$

Besides the biological metrics evaluating the optimality of sequences, we designed several metrics to quantify the differences between original and optimized RNA sequences and assess the error rate. Here, we introduce four metrics: **length error rate(LER)**, **codon error rate(CER)**, **codon error percentage(CEP)**, and **sequence difference percentage(SDP)**.

First, the length error means the length of optimized mRNA sequences differs from the original ones, indicating the missing and extra codons, which are the most common and usually seen in probabilistic models. To depict this error, we assume the number of sequences and sequences with wrong length to be  $N$  and  $N_{LE}$ , and the **length error rate (LER)** can be formulated as eq.5.

$$LER = \frac{N_{LE}}{N}. \quad (5)$$

The **codon error rate (CER)** can exhibit the proportion that sequences with wrong codons take among all sequences. Meanwhile, the **codon error percentage (CEP)** can show the average percentage of wrong codons. We assume there are  $N_{CE}$  out of  $N$  RNA sequences having codons that do not conform to the original coding aa, and  $ce_i$  of  $n_i$  codons in the  $i$ -th RNA sequence are wrong for  $i \in [1, N_{CE}]$ . The computation of the CER and CEP is shown in eq.6 and eq.7.

$$CER = \frac{N_{CE}}{N}. \quad (6)$$

$$CEP = \frac{\sum_i^{N_{CE}} ce_i}{\sum_i^{N_{CE}} n_i}. \quad (7)$$

The **Sequence Difference Percentage (SDP)** quantifies the disparity between optimized and original RNA sequences. It exhibits how much the sequence is modified. We use the  $N_{NE}$  to represent the number of RNA sequences that have no length and codon error to exclude the impact of length and codon error sequences in this metric. The relation can be formulated as  $N = N_{LE} + N_{CE} + N_{NE}$ . Subsequently, we assume there are  $sd_j$  of  $n_j$  codons in the  $i$ -th RNA sequence that are different but not wrong for  $j \in [1, N_{NE}]$ . The calculation of SDP is shown in eq.8.

$$SDP = \frac{\sum_j^{N_{NE}} sd_j}{\sum_j^{N_{NE}} n_j}. \quad (8)$$

We note that when the LER is not 0, the CER, CEP, and SDP are calculated excluding the sequences with length error. This is straightforward to understand: when the length of the original and optimized sequences is different, it is impossible to calculate whether one codon is wrong.

**Table 1:** Sequence error and difference rates (%) of RNop model for "human" with different GPLoss weight

Metrics	loss weight of GPLoss (%)							
	$10^{-6}$	$10^{-5}$	$10^{-4}$	$10^{-3}$	$10^{-2}$	$10^{-1}$	1	
LER	99.75	99.74	64.94	6.3933	0.0433	0.0	0.0	
CER	92.02	91.29	32.56.0	0.12	0.03	0.0	0.0	
CEP	25.47	25.33	1.47	0.02	0.001	0.0	0.0	
SDP	98.12	97.54	69.16	62.19	61.30	61.21	60.70	

## 4 Computational Experiments

Although the expression rate is intended to be assessed via biological experiments, to avoid the unnecessary expenditure of experimental resources and time, we initially conducted comprehensive quantitative analyses using computational methods. Consequently, experiments were carried out to evaluate the efficacy of the proposed models.

### 4.1 Mutation Regulation

The primary objective of the proposed GPLoss is to regulate the RNop model in codon generation within the correct range.

We have discussed how the mutation rate of optimized RNA sequences can be influenced by adjusting the loss weight of GPLoss in Section 3.2. To investigate this, we conducted experiments using different loss weights of GPLoss ranging from 1 to  $10^{-6}$ , focusing on the "human" model.

The results, summarized in Table 1, reveal that higher loss weights ensure that the coding proteins of the given RNA sequences remain unchanged after optimization. When the loss weight of GPLoss is over  $10^{-2}$ , the mutation rate is strictly controlled, and neither codon error nor length error appears. Conversely, as the loss weights decrease, the mutation rate for proteins increases. As the loss weight drops to  $10^{-6}$ , most sequences have the length error or codon error, indicating the existence of mutations.

Additionally, while GPLoss effectively ensures the sequence fidelity, this approach is not entirely rigid. By fine-tuning the loss weights, we can regulate the mutation rate of coding proteins for a given RNA sequence by loss weights of other loss functions.

### 4.2 Improving CAI and tAI

After ensuring that the model can accurately modify codons, our next experiment aims to evaluate the impact of the proposed RNop model on the CAI and tAI of mRNA sequences.

We apply our RNop model to the gene sequence data with different species parameters. Then we test the model and calculate the CAI and tAI for both the original and optimized RNA sequences to validate the effectiveness of our models and loss functions. The calculation process adheres to the methodology outlined in the original

**Table 2:** CAI and tAI of original and optimized mRNA

Target Species	Metrics			
	Original CAI	Optimized CAI	Original tAI	Optimized tAI
human	0.7029	0.9735	10.945	13.16
mouse	0.7003	0.9883	8.627	11.23
yeast	0.6404	0.9945	5.433	9.731
ecoli	0.6552	0.9922	1.679	2.109

**Table 3:** CAI and tAI elevation of mRNA from different species when the model optimizing species is E. coli

Original Species:	Target Species: E. coli			
	Base CAI	CAI	Base tAI	tAI
human	0.6206	0.9850	1.615	2.109
mouse	0.618	0.9847	1.614	2.105
E.coli	0.7338	0.9811	1.851	2.111
virus	0.6666	0.9774	1.737	2.182

**Table 4:** CAI and tAI elevation of mRNA from different species when the model optimizing species is human

Original Species:	Target Species: human			
	Base CAI	CAI	Base tAI	tAI
human	0.7550	0.9746	11.40	12.98
mouse	0.7450	0.9750	11.43	13.0
E.coli	0.6879	0.9730	11.04	13.2
virus	0.6755	0.9770	11.12	13.74

paper[4, 6, 7] , utilizing parameters collected from the source mentioned in Sections 3.3 and 3.4.

The results are summarized in Table 2. Notably, the optimized RNA sequences exhibit higher CAI and tAI values in the experiments conducted for the corresponding species. Given a specified species, the RNop model can optimize the sequence CAI and tAI for sequences from all resources. The optimization is universal, we can demonstrate this by assuming we are optimizing the mRNA for E. coli: we divide the test dataset into species, and we can find that the CAI and tAI of mRNA sequences originally from E. coli are also optimized. The results are shown in Table.3.

Furthermore, we also illustrate the CAI and tAI distribution using box graphs, which are shown in Fig.5, 6, 8, and 7. We tested the optimization models for "human", "ecoli", and "mouse" as a demonstration. We can observe from the figures that the optimized mRNA has better CAI and tAI than the original ones, which indicates our models succeed in raising both factors. The distribution of CAI and tAI is mainly near the average.

**Table 5:** CAI and tAI elevation of mRNA from different species when the model optimizing species is mouse

Original Species:	Target Species: mouse			
	Base CAI	CAI	Base tAI	tAI
human	0.7553	0.9528	8.985	10.89
mouse	0.7569	0.9530	9.018	10.90
E.coli	0.6308	0.9424	8.747	10.74
virus	0.6685	0.9588	8.446	11.09

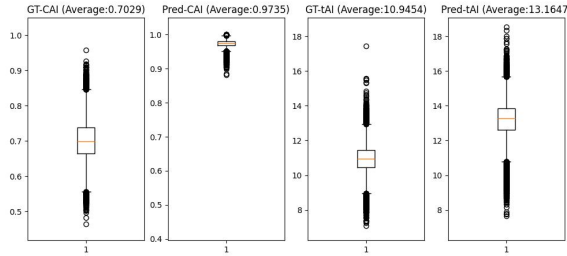


**Fig. 5:** The box graph of CAI and tAI of original and optimized RNA sequences with "human" species parameters. Optimized RNA sequences have higher mean CAI and tAI.

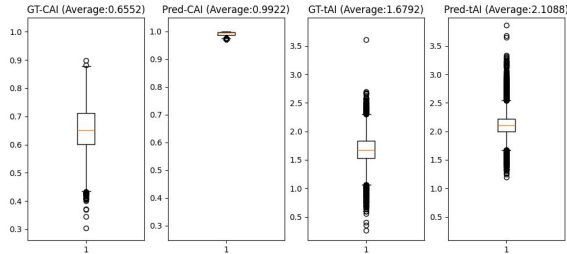


**Fig. 6:** The box graph of CAI and tAI of original and optimized RNA sequences with "ecoli" species parameters. Optimized RNA sequences have higher mean CAI and tAI.

### 4.3 Improving the MFE

As we discussed in Sec.1, the MFE can profoundly affect the stability of RNA and the efficiency of translation. Therefore, we compute the MFE of optimized sequences obtained from models with and without MFEloss.

The results are shown in Fig.9, 10, and 11. The most significant comparison is in the "yeast" experiments in Fig.11, which shows the model without the MFEloss

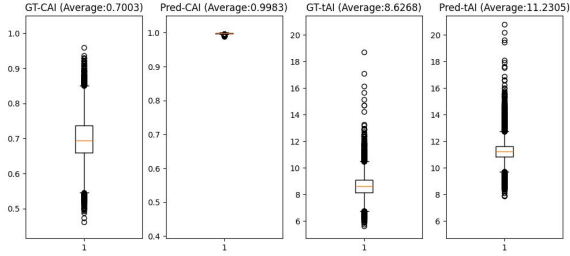


**Fig. 7: The box graph of CAI and tAI of original and optimized RNA sequences with "mouse" species parameters. Optimized RNA sequences have higher mean CAI and tAI.**

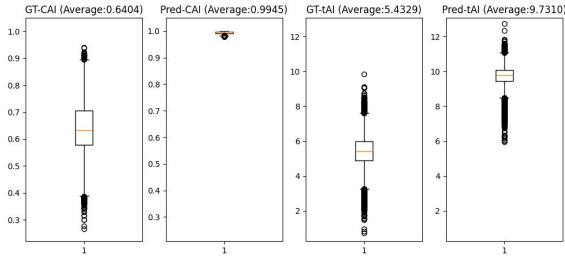


**Fig. 8: The box graph of CAI and tAI of original and optimized RNA sequences with "yeast" species parameters. Optimized RNA sequences have higher mean CAI and tAI.**

produces sequences with even higher MFE (red line) than the original ones (green line), but the model with the MFEloss can improve their MFE (blue line) better than the original ones. The results of "human" and "ecoli" are less significant. The MFE of sequences from the MFEloss-optimized model is the lowest, while the MFE from the model without MFEloss is slightly lower than the original ones, which follows the finding of Presnyak et. al[58].

## 5 Biological Experiments

After our approach for gene expression optimization is validated through computational experiments, we conduct biological experiments to further prove its effectiveness in biology.

Preliminarily, we set out to validate the efficacy of the optimization model. Therefore, we conducted experiments to showcase that the RNop model trained with the GPLoss family could produce high-expression mRNA while maintaining the protein function.

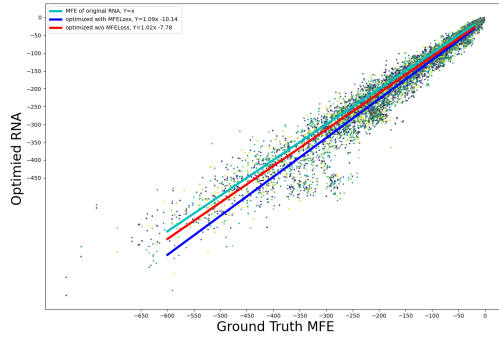


**Fig. 9: The free energy drop of optimized DNA CDS sequences in "human" species experiment.** The mint green line represents the regression results of the original RNA sequences, while the red line and blue line represent the optimized DNA CDS without and with MFEloss separately. The MFEloss-introduced optimization can further reduce the minimal free energy of DNA CDS sequences.

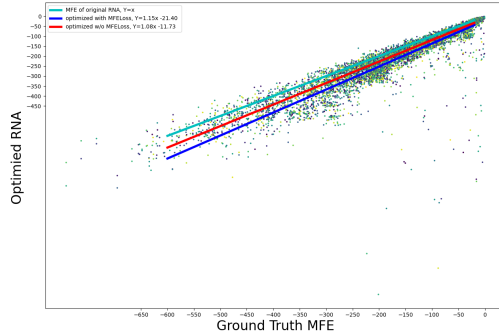


**Fig. 10: The free energy drop of optimized DNA CDS sequences in "ecoli" species experiment.** Like in the "human" species experiments, the MFEloss-introduced optimization can further reduce the minimal free energy of DNA CDS sequences.

### 5.1 Experiment 1: eGFP optimization

To better demonstrate the generalizability and ensure replicability, we use the most common fluorescence protein, the eGFP, enhanced Green Fluorescent Protein. The tested mRNA (DNA CDS) sequences of eGFP are original and optimized using our approach. We applied different models with various loss weights in this set of experiments, trying to find the best model for eGFP optimization. The "NC" represents the neutral comparison. The "HO" represents the original eGFP sequence, which has

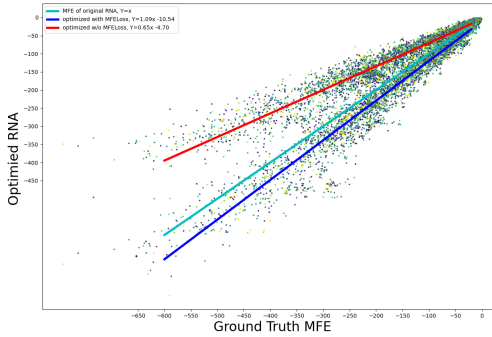


**Fig. 11: The free energy drop of optimized DNA CDS sequences in "yeast" species experiment.** The efficacy of the MFEloss is significant. The optimization without MFEloss will lead to DNA CDS sequences of higher free energy, while the optimization can reduce the minimal free energy.

already been optimized for high expression in human cells. The "HF", "HT", "HC1", and "HC2" represent the sequences optimized by RNop models with balanced loss weights, 10 times higher tAILoss loss weight, 10 times higher CAILoss loss weight, and 100 times higher CAILoss loss weight, respectively.

The fluorescence intensity and 500nm peak of fluorescence spectrophotometry were measured for the green fluorescence. The results are shown in Figure.12 and Figure.13. The higher fluorescence is generally related to higher expression of eGFP, which can be compared through these figures.

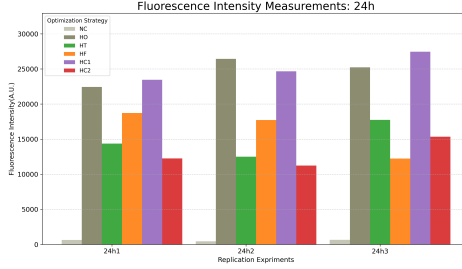
Through these experiments, we can summarize the following points of the RNop models.

1. The results show that the RNop models have ensured the expression and function of eGFP are preserved. It indicates that the RNop models are efficacy for mRNA optimization while retaining good fidelity.
2. The comparison of results from original sequences and optimized sequences demonstrates that most sequences optimized by RNop models have better expression, indicating their effectiveness.
3. For eGFP, the highest expression sequence is optimized by the HC1 RNop model. It shows that the optimality of mRNA sequences is not only related to the optimization factors, but also to the sequences themselves.

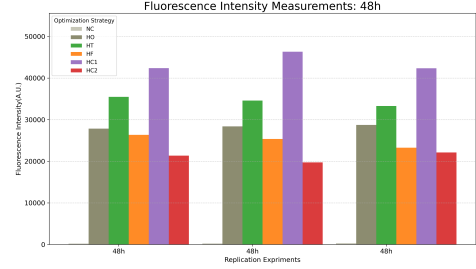
## 6 Discussion

### 6.1 Cornerstone Model Architecture

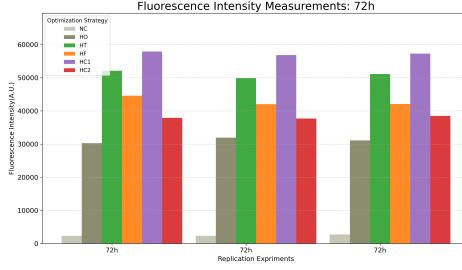
Since the network architecture will influence the data-driven and knowledge-based models, we also have a pathway when we are exploring the different models. The results of different models are hard to present in quantitative metrics.



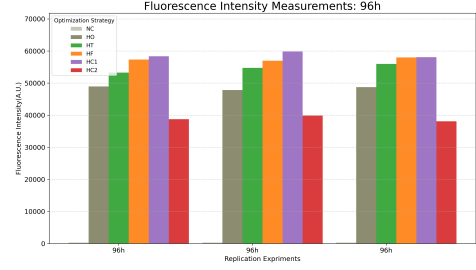
(a) The results of fluorescence intensity (A.U.) at 24 hours.



(b) The results of fluorescence intensity (A.U.) at 48 hours.



(c) The results of fluorescence intensity (A.U.) at 72 hours.



(d) The results of fluorescence intensity (A.U.) at 96 hours.

**Fig. 12: The results of biological validation experiments: fluorescence intensity (A.U.).** We applied different models to the eGFP sequence. "NC": neutral comparison, "HO": original eGFP sequence, "HF": optimized with balanced loss weights, "HT":  $10 \times$  tAI Loss weight, "HC1":  $10 \times$  CAI Loss weight, and "HC2":  $100 \times$  CAI Loss weight. To ensure consistency, 3 replications are conducted.

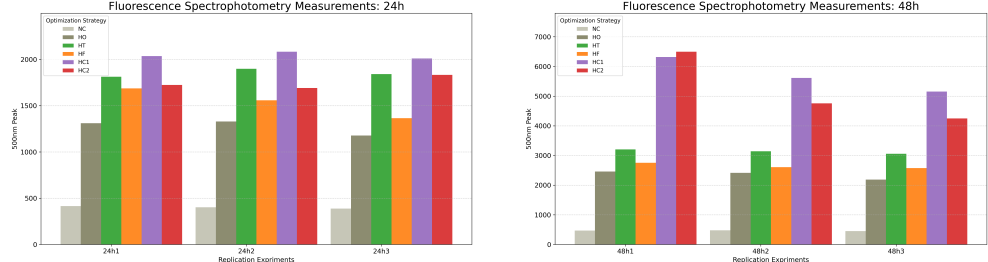
### Linear Model:

In the preliminary stages, we applied pure linear networks like MLP[59, 60]. The applied linear models have the same hidden sizes in each linear layer, with normalization and activation layers behind every two linear layers.

Though the linear models achieve good outcomes in the MFE Loss, they suffer from severe overfitting in mRNA optimization. Most attempts with linear models result in sequences with high LER (defined in Equation.5) up to 99%, which is unacceptable. We tried to improve their performance but failed. However, in this seemingly hopeless first attempt, we observed that the GPLoss is functional at the beginning of the training stage. The LER dropped at first and then rose, and the mRNA sequences with correct length have competitively low CER (defined in Eq.6). This phenomenon let us know the CAI Loss worked and gave us hope for subsequent experiments.

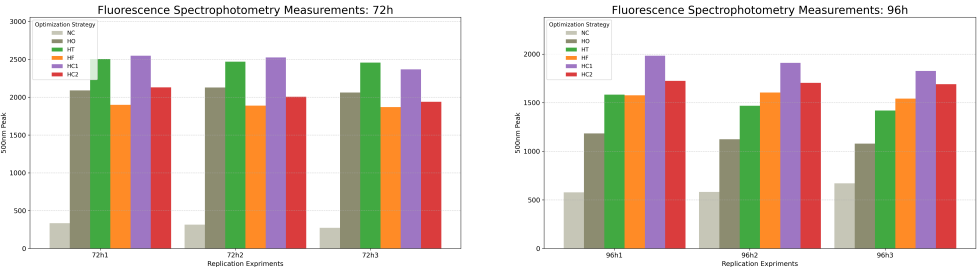
### Sequence to Sequence Model:

The RNN and LSTM models are common models for sequence-to-sequence tasks, also including codon optimization[19, 20]. We applied LTSMS models with the GPLoss



(a) The 500 nm peak measurement results of fluorescence spectrophotometry at 24 hours.

(b) The 500 nm peak measurement results of fluorescence spectrophotometry at 48 hours.



(c) The 500 nm peak measurement results of fluorescence spectrophotometry at 72 hours.

(d) The 500 nm peak measurement results of fluorescence spectrophotometry at 96 hours.

**Fig. 13: The results of biological validation experiments: fluorescence spectrophotometry.** The naming is the same as the fluorescence intensity experiments. The 500nm peak is measured for the green fluorescence of eGFP. To ensure consistency, 3 replications are conducted.

family to optimize the mRNA sequences. However, the process length of LTSM models can not support the proposed MFEloss. The MFE of mRNA sequences can be calculated by algorithms or predicted by deep learning models using the full-length sequences, while during the processing of LSTM models, there are fragments of sequences. Therefore, the LSTM models with the GPLoss family without the MFEloss demonstrated the effectiveness of CAILoss and tAIloss. The optimized sequences exhibit high CAI and tAI, and obtain slight optimization in MFE, which is similar to that we have shown in Section 4.3. The results of LSTM models are competitive, but we still want to fully leverage the loss functions we have designed. We then turn to try other models to optimize the whole sequence.

#### Language Model and Transformer:

One prominent example of the Transformer-based language model is BERT[31]. The codonBert[32] has been proposed for RNA-related tasks. Therefore, this model was among the first that we considered during the initial stages of integrating language

modeling and Transformer architectures for this task. Therefore, we used BERT at first to design the tokenizer and embedding methods. Generally, the embedding of BERT consists of word, position, and segment embedding, while we need only the word and position embedding in mRNA optimization because the mRNA data is preferred to be inputted solely for convenience in loss computing.

For this task, we employed the BertSequenceToSequence model, incorporating modified tokenization and embedding methods. The results indicate that the extensive number of parameters in BERT renders the model susceptible to overfitting at the very early stages of training.

Subsequently, we evaluated a pure Transformer model, similar to our earlier attempts with linear models. It is widely acknowledged that Transformers excel in sequence-to-sequence tasks, as evidenced by models such as TransformerXL[61] and T5[62]. Therefore, in this experiment, we utilized the T5Block while maintaining the same embedding methods as used in the BERT experiment. Unfortunately, the results were unsatisfactory, with overfitting continuing to pose a challenge during the later stages of training. However, the model with fewer parameters and layers shed light on our next exploration. This model was more stable than the larger ones and had the lowest LER in one of its training results.

#### **Vision Transformer:**

After the attempts with Transformer and Language models, we realized that the Transformer might be a promising pathway for stable mRNA sequence optimization. The problem then was how to reduce the parameters and model size while keeping its global dependency and model complexity. As we discussed in the sections above, the lack of global dependency or not regarding the mRNA as an integral whole may cause trouble in improving MFE. Vision Transformer models are good candidates due to their low parameter amount and model complexity. Meanwhile, there are many modified versions of ViT[53, 54] for better global and long-term dependency, which can avoid processing the mRNA sequences as independent parts.

We then regard the mRNA optimization task as a vision task. The mRNA sequence data, which is a 2-dimensional matrix as we discussed in Section 3.2, can be divided into fragments of the same length with input projection size. This step makes the mRNA sequence feature akin to a multi-dimensional image with equal height and width. Thus, we can use the Vision Transformer to process sequence data.

After preliminary tests, we found the results were surprisingly good. The length error was almost prevented, and all loss functions worked functionally. The codon error appeared at first and vanished after we raised the GPLoss weight. Finally, the mRNA sequences coding correct proteins with higher CAI, tAI, and MFE were obtained by these models. Therefore, the Vision Transformer models are selected for this task.

## **6.2 Ablation Study**

### **6.2.1 Loss Weights**

Besides the experiments with loss weight changes, we also conduct numerous experiments to showcase the effect of loss weights on the optimization results. The GPLoss is the foundation loss function for the model, and we have tested different loss weights

**Table 6:** CAI, tAI, and average MFE of mRNA sequences optimized by models with different CAILoss loss weights

Loss weight multiplier	CAI	tAI	MFE
100×	1.00	13.63	-45.62
10×	0.9983	13.64	-49.80
1×	0.9895	13.69	-52.87
0.1×	0.7720	11.50	-14.69
0.01×	0.7614	11.64	-2.96

**Table 7:** CAI, tAI, and average MFE of mRNA sequences optimized by models with different tAILoss loss weights

Loss weight multiplier	CAI	tAI	MFE
100×	0.9503	13.13	-40.61
10×	0.9606	12.86	-43.86
1×	0.9895	13.69	-52.87
0.1×	0.9506	13.14	-40.35
0.01×	0.9795	13.24	-52.64

in Section 4.1. Therefore, in this ablation study, we will not conduct the redundant experiments in GPLoss weights and will focus on the other loss functions.

The loss weight was adjusted using multipliers. Specifically, the  $100\times$  indicates that the loss weight is increased by a factor of 100 during training. In these experiments, both CAILoss and tAILoss were evaluated with loss weight multipliers ranging from  $0.01\times$  to  $100\times$ . The results are presented in Table ???. As illustrated in the chart, mostly, an increase in the loss weight for either CAILoss or tAILoss leads to a slight improvement in the optimized CAI and tAI values, while other performance metrics exhibit a corresponding decline.

However, this trend was not consistently observed across all experiments that were conducted. When the loss weight is set to  $0.01\times$  or  $100\times$ , the unbalanced loss values may cause unstable convergence. The loss weight we chose for the RNop model is adequate for both loss functions to contribute equally to the learning process and thus reach the best performance.

### 6.2.2 MFEloss Ratio

In Section 3.5, we mentioned a parameter  $\lambda$  to ensure the optimization target is higher than the original MFE. In this ablation study, we conduct several experiments with models trained with MFEloss in different MFEloss Ratios,  $\lambda$ . The other loss functions are retained, while the  $\lambda$  of MFEloss is adjusted from 0.9 to 1.5.

The results are shown in Table 8. We can observe from the table that the  $\lambda = 1.1$ , which is used in the MFEloss, is the optimal value for the balance of MFE improvement and sequence stability. When the  $\lambda$  is too high, the model can hardly optimize the mRNA sequences to such MFE, resulting in a high MFEloss value across the training stage and competing between the GPLoss and MFEloss. This then causes

**Table 8:** LER, CAI, tAI, and average MFE of mRNA sequences optimized by MFEloss with different MFEloss Ratios

MFEloss Ratio $\lambda$	Metrics			
	LER	CAI	tAI	MFE
0.9	0.0	0.9795	13.24	-48.93
1.0	0.0	0.9821	13.02	-46.54
1.1	0.0	0.9895	13.69	-52.87
1.25	0.0	0.9739	13.12	-47.96
1.5	0.0267	0.9370	12.61	-27.76

the length error and codon error in optimized mRNA sequences, which is seen in the  $\lambda = 1.5$  experiment. When the  $\lambda$  is too low, the model will not actively optimize the MFE. Therefore, corresponding sequences have relatively higher MFE than sequences from the RNop model where  $\lambda = 1.1$ .

### 6.3 Computation speed

The conventional methods in mRNA (or DNA CDS) optimization like DP have a high time complexity  $O(n^3)$ [16, 63], which will cause burdensome time consumption when processing sequences over 2000 bps. Even the faster method, like LinearDesign[17], has the  $O(n^2)$  time complexity. Their processing time is usually high when the length of the mRNA sequences is over 3000 (in base pairs).

On the contrary, the processing time of our model is directly related to the maximum sequence length, which will not change after the training process. When the input length is fixed, as long as the sequence length is under the model capacity, the sequences will have the same processing time in a batch. Therefore, for most situations, there is a great advantage of neural network methods for their low time consumption and batch computation

We test the reference time of our methods with different parameter quantities and sequence lengths. The results are shown in Table.9. In comparison, the CDSFold[16] takes about 1 h to design a CDS of length 2.7 kbp. Meanwhile, the time consumption of the LinearDesign to optimize a 1000 bps mRNA is over minutes. Even the linear approximation of LinearDesign is far more time-consuming than our neural network methods. The models with larger parameter amounts dealing with longer sequences also achieve better performance compared to the algorithm-based methods.

The high process speed enables the possibility of high-throughput analysis in mRNA design by optimizing the mRNA for high expression while keeping its encoded protein with the same function and similar structure. The models can be combined with protein structure and function prediction models. Besides, using the GPLoss loss function family has a unique advantage in simultaneously reaching a high protein expression rate and regulating the mutation rate freely. This can be problematic to achieve for algorithm-based methods: they usually limit the searching range within the codons of coded amino acids.

**Table 9:** Time consumption under different situations (seq/s)

Hidden Size & Depth	Max Sequence Length		
	3072	6144	9216
1024 × 16	47.32	29.76	24.61
2048 × 16	33.28	28.87	22.60
4096 × 24	21.66	15.57	10.56

With faster process speed, higher customization flexibility, and potential for further exploration, the Gene-Protein loss function family can profoundly boost deep-learning-based mRNA optimization methods.

#### 6.4 Limitations

We recognize other critical factors that can impact the mRNA translation process, like the MTDR (mean of typical decoding rate). Our work has not yet incorporated these factors. We are actively exploring ways to bridge the gap between biological terminology and computational language, aiming to translate them into optimization factors for deep learning methods.

### 7 Conclusion

In this paper, we propose **RNop** to address the desired optimization features for mRNA sequences simultaneously, including high fidelity, low computational cost, and the various scopes of optimization variables considering the mRNA whole lifecycle. The RNop comprehensively incorporates the factors related to the mRNA lifecycle and translation process, including intrinsic mRNA sequence properties, secondary structure, translation elongation kinetics, and tRNA availability. Four specialized loss functions, the GPLoss, CAIloss, tAIloss, and MFEloss, were proposed to enable explicit control over sequence fidelity, codon adaptation optimization, tRNA availability promotion, and mRNA secondary structure enhancement. Then, we demonstrate RNop’s efficacy and effectiveness through extensive in silico and in vivo experiments. RNop ensures high sequence fidelity, achieves significant computational throughput up to 47.32 sequences/s. It extends the horizon significantly for the mRNA optimization. We plan to engage more optimization factors and include more species parameters in RNop in the future. The data and model will be released for further research.

### Acknowledgements

**Competing interests:** The author(s) declare no competing interests.

### Author contributions statement

**Zheng Gong:** Conceptualization, Methodology, Validation, Data Curation, Writing - Original Draft, Visualization. **Ziyi Jiang:** Conceptualization, Validation, Writing -

Review and Editing. **Weihao Gao:** Conceptualization, Writing - Review and Editing. **Zhuo Deng:** Writing - Review and Editing. **Lan Ma:** Funding acquisition, Supervision.

## Availability of Data and Materials

The data and code are available at <https://github.com/HudenJear/RPLoss> for justified usage and research upon request. Please contact the corresponding author if you have any questions about the data and code.

## References

- [1] Jain, R., Jain, A., Mauro, E., LeShane, K., Densmore, D.: Icor: improving codon optimization with recurrent neural networks. *BMC Bioinformatics* **24**(1), 132 (2023) <https://doi.org/10.1186/s12859-023-05246-8>
- [2] Paremskaia, A.I., Kogan, A.A., Murashkina, A., Naumova, D.A., Satish, A., Abramov, I.S., Feoktistova, S.G., Mityaeva, O.N., Deviatkin, A.A., Volchkov, P.Y.: Codon-optimization in gene therapy: promises, prospects and challenges. *Front Bioeng Biotechnol* **12**, 1371596 (2024)
- [3] Buhr, F., Jha, S., Thommen, M., Mittelstaet, J., Kutz, F., Schwalbe, H., Rodnina, M.V., Komar, A.A.: Synonymous codons direct cotranslational folding toward different protein conformations. *Molecular Cell* **61**(3), 341–351 (2016) <https://doi.org/10.1016/j.molcel.2016.01.008>
- [4] Sharp, P.M., Li, W.-H.: The codon adaptation index-a measure of directional synonymous codon usage bias, and its potential applications. *Nucleic Acids Research* **15**(3), 1281–1295 (1987) <https://doi.org/10.1093/nar/15.3.1281> <https://academic.oup.com/nar/article-pdf/15/3/1281/3988268/15-3-1281.pdf>
- [5] Courel, M., Clément, Y., Bossevain, C., Foretek, D., Vidal Cruchez, O., Yi, Z., Bénard, M., Benassy, M.-N., Kress, M., Vindry, C., Ernoult-Lange, M., Antoniewski, C., Morillon, A., Brest, P., Hubstenberger, A., Roest Crolius, H., Standart, N., Weil, D.: GC content shapes mRNA storage and decay in human cells. *Elife* **8** (2019)
- [6] Reis, M., Wernisch, L., Savva, R.: Unexpected correlations between gene expression and codon usage bias from microarray data for the whole escherichia coli K-12 genome. *Nucleic Acids Res* **31**(23), 6976–6985 (2003)
- [7] Reis, M.d., Savva, R., Wernisch, L.: Solving the riddle of codon usage preferences: a test for translational selection. *Nucleic Acids Research* **32**(17), 5036–5044 (2004) <https://doi.org/10.1093/nar/gkh834> <https://academic.oup.com/nar/article-pdf/32/17/5036/4156320/gkh834.pdf>
- [8] Mathews, D.H., Disney, M.D., Childs, J.L., Schroeder, S.J., Zuker, M., Turner, D.H.: Incorporating chemical modification constraints into a dynamic programming algorithm for prediction of rna secondary structure. *Proceedings of the National Academy of Sciences* **101**(19), 7287–7292 (2004) <https://doi.org/10.1073/pnas.0401799101> <https://www.pnas.org/doi/pdf/10.1073/pnas.0401799101>
- [9] Mathews, D.H., Sabina, J., Zuker, M., Turner, D.H.: Expanded sequence dependence of thermodynamic parameters improves prediction of rna secondary structure11edited by i. tinoco. *Journal of Molecular Biology* **288**(5), 911–940 (1999) <https://doi.org/10.1006/jmbi.1999.2700>

[10] Mathews, D.H., Disney, M.D., Childs, J.L., Schroeder, S.J., Zuker, M., Turner, D.H.: Incorporating chemical modification constraints into a dynamic programming algorithm for prediction of rna secondary structure. *Proceedings of the National Academy of Sciences* **101**(19), 7287–7292 (2004) <https://doi.org/10.1073/pnas.0401799101> <https://www.pnas.org/doi/pdf/10.1073/pnas.0401799101>

[11] Dana, A., Tuller, T.: Mean of the typical decoding rates: A new translation efficiency index based on the analysis of ribosome profiling data. *G3 Genes—Genomes—Genetics* **5**(1), 73–80 (2015) <https://doi.org/10.1534/g3.114.015099> <https://academic.oup.com/g3journal/article-pdf/5/1/73/37191150/g3journal0073.pdf>

[12] Vaidyanathan, S., Azizian, K.T., Haque, A.K.M.A., Henderson, J.M., Hendel, A., Shore, S., Antony, J.S., Hogrefe, R.I., Kormann, M.S.D., Porteus, M.H., McCaffrey, A.P.: Uridine depletion and chemical modification increase cas9 mRNA activity and reduce immunogenicity without HPLC purification. *Mol Ther Nucleic Acids* **12**, 530–542 (2018)

[13] Vostrosablin, N., Lim, S., Gopal, P., Brazdilova, K., Parajuli, S., Wei, X., Gromek, A., Prihoda, D., Spale, M., Muzdalo, A., Greig, J., Yeo, C., Wardyn, J., Mejzlik, P., Henry, B., Partridge, A.W., Bitton, D.A.: mrnaid, an open-source platform for therapeutic mrna design and optimization strategies. *NAR Genomics and Bioinformatics* **6**(1), 028 (2024) <https://doi.org/10.1093/nargab/lqae028> <https://academic.oup.com/nargab/article-pdf/6/1/lqae028/56958324/lqae028.pdf>

[14] Zulkower, V., Rosser, S.: Dna chisel, a versatile sequence optimizer. *Bioinformatics* **36**(16), 4508–4509 (2020) <https://doi.org/10.1093/bioinformatics/btaa558> <https://academic.oup.com/bioinformatics/article-pdf/36/16/4508/50676819/btaa558.pdf>

[15] GenScript: GenSmart™ Codon Optimization Tool. Accessed: 2025-02-19 (2025). <https://www.genscript.com/tools/gensmart-codon-optimization>

[16] Terai, G., Kamegai, S., Asai, K.: Cdsfold: an algorithm for designing a protein-coding sequence with the most stable secondary structure. *Bioinformatics (Oxford, England)* **32**(6), 828–834 (2016) <https://doi.org/10.1093/bioinformatics/btv678>

[17] Zhang, H., Zhang, L., Lin, A., Xu, C., Li, Z., Liu, K., Liu, B., Ma, X., Zhao, F., Jiang, H., Chen, C., Shen, H., Li, H., Mathews, D.H., Zhang, Y., Huang, L.: Algorithm for optimized mrna design improves stability and immunogenicity. *Nature* **621**(7978), 396–403 (2023) <https://doi.org/10.1038/s41586-023-06127-z>

[18] Bixi, G., Durrant, M.G., Ku, J., Poli, M., Brockman, G., Chang, D., Gonzalez, G.A., King, S.H., Li, D.B., Merchant, A.T., Naghipourfar, M., Nguyen,

E., Ricci-Tam, C., Romero, D.W., Sun, G., Taghibakshi, A., Vorontsov, A., Yang, B., Deng, M., Gorton, L., Nguyen, N., Wang, N.K., Adams, E., Baccus, S.A., Dillmann, S., Ermon, S., Guo, D., Ilango, R., Janik, K., Lu, A.X., Mehta, R., Mofrad, M.R.K., Ng, M.Y., Pannu, J., Ré, C., Schmok, J.C., John, J.S., Sullivan, J., Zhu, K., Zynda, G., Balsam, D., Collison, P., Costa, A.B., Hernandez-Boussard, T., Ho, E., Liu, M.-Y., McGrath, T., Powell, K., Burke, D.P., Goodarzi, H., Hsu, P.D., Hie, B.L.: Genome modeling and design across all domains of life with evo 2. *bioRxiv* (2025) <https://doi.org/10.1101/2025.02.18.638918> <https://www.biorxiv.org/content/early/2025/02/21/2025.02.18.638918.full.pdf>

[19] Fu, H., Liang, Y., Zhong, X., Pan, Z., Huang, L., Zhang, H., Xu, Y., Zhou, W., Liu, Z.: Codon optimization with deep learning to enhance protein expression. *Scientific Reports* **10**(1), 17617 (2020) <https://doi.org/10.1038/s41598-020-74091-z>

[20] Goulet, D.R., Yan, Y., Agrawal, P., Waight, A.B., Mak, A.N.-s., Zhu, Y.: Codon optimization using a recurrent neural network. *Journal of Computational Biology* **30**(1), 70–81 (2023) <https://doi.org/10.1089/cmb.2021.0458> <https://doi.org/10.1089/cmb.2021.0458>. PMID: 35727687

[21] Taneda, A., Asai, K.: Cosmo: A dynamic programming algorithm for multicriteria codon optimization. *Computational and Structural Biotechnology Journal* **18**, 1811–1818 (2020) <https://doi.org/10.1016/j.csbj.2020.06.035>

[22] Babjac, A.N., Lu, Z., Emrich, S.J.: Codonbert: Using bert for sentiment analysis to better predict genes with low expression. In: *Proceedings of the 14th ACM International Conference on Bioinformatics, Computational Biology, and Health Informatics. BCB '23*. Association for Computing Machinery, New York, NY, USA (2023). <https://doi.org/10.1145/3584371.3613013> . <https://doi.org/10.1145/3584371.3613013>

[23] Park, Y.S., Seo, S.W., Hwang, S., Chu, H.S., Ahn, J.-H., Kim, T.-W., Kim, D.-M., Jung, G.Y.: Design of 5'-untranslated region variants for tunable expression in escherichia coli. *Biochemical and Biophysical Research Communications* **356**(1), 136–141 (2007) <https://doi.org/10.1016/j.bbrc.2007.02.127>

[24] Xiao, J., Peng, B., Su, Z., Liu, A., Hu, Y., Nomura, C.T., Chen, S., Wang, Q.: Facilitating protein expression with portable 5'-utr secondary structures in bacillus licheniformis. *ACS Synthetic Biology* **9**(5), 1051–1058 (2020) <https://doi.org/10.1021/acssynbio.9b00355>

[25] Yi, J.S., Kim, M.W., Kim, M., Jeong, Y., Kim, E.-J., Cho, B.-K., Kim, B.-G.: A novel approach for gene expression optimization through native promoter and 5' utr combinations based on rna-seq, ribo-seq, and tss-seq of streptomyces coelicolor. *ACS Synthetic Biology* **6**(3), 555–565 (2017) <https://doi.org/10.1021/acssynbio.6b00263>

[26] Saito, Y., Kitagawa, W., Kumagai, T., Tajima, N., Nishimiya, Y., Tamano, K.,

Yasutake, Y., Tamura, T., Kameda, T.: Developing a codon optimization method for improved expression of recombinant proteins in actinobacteria. *Scientific Reports* **9**(1), 8338 (2019) <https://doi.org/10.1038/s41598-019-44500-z>

- [27] Mathews, D.H., Andre, T.C., Kim, J., Turner, D.H., Zuker, M.: An Updated Recursive Algorithm for RNA Secondary Structure Prediction with Improved Thermodynamic Parameters. *ACS Symposium Series*, vol. 682, pp. 246–257. American Chemical Society, ??? (1997). <https://doi.org/10.1021/bk-1998-0682.ch015> . 0. <https://doi.org/10.1021/bk-1998-0682.ch015>
- [28] Reuter, J.S., Mathews, D.H.: Rnastructure: software for rna secondary structure prediction and analysis. *BMC Bioinformatics* **11**(1), 129 (2010) <https://doi.org/10.1186/1471-2105-11-129>
- [29] Kierzek, E., Zhang, X., Watson, R.M., Kennedy, S.D., Szabat, M., Kierzek, R., Mathews, D.H.: Secondary structure prediction for rna sequences including n6-methyladenosine. *Nature Communications* **13**(1), 1271 (2022) <https://doi.org/10.1038/s41467-022-28817-4>
- [30] Gong, H., Wen, J., Luo, R., Feng, Y., Guo, J., Fu, H., Zhou, X.: Integrated mrna sequence optimization using deep learning. *Briefings in Bioinformatics* **24**(1), 001 (2023) <https://doi.org/10.1093/bib/bbad001> <https://academic.oup.com/bib/article-pdf/24/1/bbad001/48782582/bbad001.pdf>
- [31] Devlin, J., Chang, M.-W., Lee, K., Toutanova, K.: BERT: Pre-training of Deep Bidirectional Transformers for Language Understanding (2019). <https://arxiv.org/abs/1810.04805>
- [32] Li, S., Moayedpour, S., Li, R., Bailey, M., Riahi, S., Kogler-Anele, L., Miladi, M., Miner, J., Zheng, D., Wang, J., et al.: Codonbert: Large language models for mrna design and optimization. *bioRxiv*, 2023–09 (2023)
- [33] Yu, H., Yang, H., Sun, W., Yan, Z., Yang, X., Zhang, H., Ding, Y., Li, K.: An interpretable rna foundation model for exploring functional rna motifs in plants. *Nature Machine Intelligence* **6**(12), 1616–1625 (2024) <https://doi.org/10.1038/s42256-024-00946-z>
- [34] Shen, T., Hu, Z., Sun, S., Liu, D., Wong, F., Wang, J., Chen, J., Wang, Y., Hong, L., Xiao, J., Zheng, L., Krishnamoorthi, T., King, I., Wang, S., Yin, P., Collins, J.J., Li, Y.: Accurate rna 3d structure prediction using a language model-based deep learning approach. *Nature Methods* **21**(12), 2287–2298 (2024) <https://doi.org/10.1038/s41592-024-02487-0>
- [35] Badia-i-Mompel, P., Vélez Santiago, J., Braunger, J., Geiss, C., Dimitrov, D., Müller-Dott, S., Taus, P., Dugourd, A., Holland, C.H.,

Ramirez Flores, R.O., Saez-Rodriguez, J.: decoupler: ensemble of computational methods to infer biological activities from omics data. *Bioinformatics Advances* **2**(1), 016 (2022) <https://doi.org/10.1093/bioadv/vbac016> <https://academic.oup.com/bioinformaticsadvances/article-pdf/2/1/vbac016/47081980/vbac016.pdf>

[36] Wessels, H.-H., Stirn, A., Méndez-Mancilla, A., Kim, E.J., Hart, S.K., Knowles, D.A., Sanjana, N.E.: Prediction of on-target and off-target activity of crispr-cas13d guide rnas using deep learning. *Nature Biotechnology* **42**(4), 628–637 (2024) <https://doi.org/10.1038/s41587-023-01830-8>

[37] Müller-Dott, S., Tsirvouli, E., Vazquez, M., Ramirez Flores, R.O., Badia-i-Mompel, P., Fallegger, R., Türei, D., Lægreid, A., Saez-Rodriguez, J.: Expanding the coverage of regulons from high-confidence prior knowledge for accurate estimation of transcription factor activities. *Nucleic Acids Research* **51**(20), 10934–10949 (2023) <https://doi.org/10.1093/nar/gkad841> <https://academic.oup.com/nar/article-pdf/51/20/10934/53175342/gkad841.pdf>

[38] Garcia-Alonso, L., Holland, C.H., Ibrahim, M.M., Turei, D., Saez-Rodriguez, J.: Benchmark and integration of resources for the estimation of human transcription factor activities. *Genome Res* **29**(8), 1363–1375 (2019)

[39] Wang, W., Feng, C., Han, R., Wang, Z., Ye, L., Du, Z., Wei, H., Zhang, F., Peng, Z., Yang, J.: trrosettarna: automated prediction of rna 3d structure with transformer network. *Nature Communications* **14**(1), 7266 (2023)

[40] Chen, J., Hu, Z., Sun, S., Tan, Q., Wang, Y., Yu, Q., Zong, L., Hong, L., Xiao, J., Shen, T., et al.: Interpretable rna foundation model from unannotated data for highly accurate rna structure and function predictions. *arXiv preprint arXiv:2204.00300* (2022)

[41] Fu, L., Cao, Y., Wu, J., Peng, Q., Nie, Q., Xie, X.: Ufold: fast and accurate rna secondary structure prediction with deep learning. *Nucleic acids research* **50**(3), 14–14 (2022)

[42] Tan, Z., Fu, Y., Sharma, G., Mathews, D.H.: Turbofold ii: Rna structural alignment and secondary structure prediction informed by multiple homologs. *Nucleic acids research* **45**(20), 11570–11581 (2017)

[43] Sloma, M.F., Mathews, D.H.: Exact calculation of loop formation probability identifies folding motifs in rna secondary structures. *RNA* **22**(12), 1808–1818 (2016)

[44] Wayment-Steele, H.K., Kladwang, W., Watkins, A.M., Kim, D.S., Tunguz, B., Reade, W., Demkin, M., Romano, J., Wellington-Oguri, R., Nicol, J.J., et al.: Deep learning models for predicting rna degradation via dual crowdsourcing. *Nature Machine Intelligence* **4**(12), 1174–1184 (2022)

[45] Das, R., Wayment-Steele, H., Kim, D.S., Choe, C., Tunguz, B., Reade, W., Demkin, M.: OpenVaccine: COVID-19 mRNA Vaccine Degradation Prediction. Kaggle (2020). <https://kaggle.com/competitions/stanford-covid-vaccine>

[46] Ding, Z., Guan, F., Xu, G., Wang, Y., Yan, Y., Zhang, W., Wu, N., Yao, B., Huang, H., Tuller, T., *et al.*: Mpepe, a predictive approach to improve protein expression in *e. coli* based on deep learning. *Computational and Structural Biotechnology Journal* **20**, 1142–1153 (2022)

[47] Diez, M., Medina-Muñoz, S.G., Castellano, L.A., Silva Pescador, G., Wu, Q., Bazzini, A.A.: icodon customizes gene expression based on the codon composition. *Scientific Reports* **12**(1), 12126 (2022)

[48] Nabeel Asim, M., Imran Malik, M., Dengel, A., Ahmed, S.: K-mer neural embedding performance analysis using amino acid codons. In: 2020 International Joint Conference on Neural Networks (IJCNN), pp. 1–8 (2020). <https://doi.org/10.1109/IJCNN48605.2020.9206892>

[49] National Center for Biotechnology Information (NCBI): NCBI Genome Database. [cited 2025 Jan 16] (1988–). <https://www.ncbi.nlm.nih.gov/datasets/genome/>

[50] GenScript: GenScript Codon Frequency Table. <https://www.genscript.com/tools/codon-frequency-table>. Accessed: 2024/07/03

[51] Chan, P.P., Lowe, T.M.: GtRNAdb 2.0: an expanded database of transfer RNA genes identified in complete and draft genomes. *Nucleic Acids Res* **44**(D1), 184–9 (2015)

[52] Zhang, J., Fei, Y., Sun, L., Zhang, Q.C.: Advances and opportunities in rna structure experimental determination and computational modeling. *Nature Methods* **19**(10), 1193–1207 (2022) <https://doi.org/10.1038/s41592-022-01623-y>

[53] Dosovitskiy, A., Beyer, L., Kolesnikov, A., Weissenborn, D., Zhai, X., Unterthiner, T., Dehghani, M., Minderer, M., Heigold, G., Gelly, S., Uszkoreit, J., Houlsby, N.: An Image is Worth 16x16 Words: Transformers for Image Recognition at Scale (2021). <https://arxiv.org/abs/2010.11929>

[54] Liu, Z., Lin, Y., Cao, Y., Hu, H., Wei, Y., Zhang, Z., Lin, S., Guo, B.: Swin transformer: Hierarchical vision transformer using shifted windows. *arXiv preprint arXiv:2103.14030* (2021)

[55] National Center for Biotechnology Information (NCBI): NCBI Virus Database. [cited 2025 Jan 16] (1988–). <https://www.ncbi.nlm.nih.gov/labs/virus/vssi/#/>

[56] Kingma, D.P., Ba, J.: Adam: A Method for Stochastic Optimization (2017). <https://arxiv.org/abs/1412.6980>

- [57] Loshchilov, I., Hutter, F.: Decoupled Weight Decay Regularization (2019). <https://arxiv.org/abs/1711.05101>
- [58] Presnyak, V., Alhusaini, N., Chen, Y.-H., Martin, S., Morris, N., Kline, N., Olson, S., Weinberg, D., Baker, K.E., Graveley, B.R., Collier, J.: Codon optimality is a major determinant of mRNA stability. *Cell* **160**(6), 1111–1124 (2015)
- [59] Kothari, S.C., Oh, H.: Neural networks for pattern recognition. *Advances in Computers*, vol. 37, pp. 119–166. Elsevier (1993). [https://doi.org/10.1016/S0065-2458\(08\)60404-0](https://doi.org/10.1016/S0065-2458(08)60404-0) . <https://www.sciencedirect.com/science/article/pii/S0065245808604040>
- [60] Tolstikhin, I.O., Houlsby, N., Kolesnikov, A., Beyer, L., Zhai, X., Unterthiner, T., Yung, J., Steiner, A., Keysers, D., Uszkoreit, J., Lucic, M., Dosovitskiy, A.: Mlp-mixer: An all-mlp architecture for vision. In: Ranzato, M., Beygelzimer, A., Dauphin, Y., Liang, P.S., Vaughan, J.W. (eds.) *Advances in Neural Information Processing Systems*, vol. 34, pp. 24261–24272. Curran Associates, Inc., ??? (2021)
- [61] Dai, Z., Yang, Z., Yang, Y., Carbonell, J., Le, Q.V., Salakhutdinov, R.: Transformer-XL: Attentive Language Models Beyond a Fixed-Length Context (2019). <https://arxiv.org/abs/1901.02860>
- [62] Raffel, C., Shazeer, N., Roberts, A., Lee, K., Narang, S., Matena, M., Zhou, Y., Li, W., Liu, P.J.: Exploring the limits of transfer learning with a unified text-to-text transformer. *Journal of Machine Learning Research* **21**(140), 1–67 (2020)
- [63] Cohen, B., Skiena, S.: Natural selection and algorithmic design of mRNA. *Journal of Computational Biology* **10**(3-4), 419–432 (2003) <https://doi.org/10.1089/10665270360688101> <https://doi.org/10.1089/10665270360688101>. PMID: 12935336